Molecular Therapy
Methods & Clinical Development
Original Article

Hexon modification of human adenovirus type 5 vectors enables efficient transduction of human multipotent mesenchymal stromal cells

Robin Nilson,[1] Olivia Lübbers,[1] Christoph Q. Schmidt,[2] Markus Rojewski,[3,4] Philip Helge Zeplin,[5] Wolfgang Funk,[6] Hubert Schrezenmeier,[3,4] Astrid Kritzinger,[1] Stefan Kochanek,[1] and Lea Krutzke[1]

[1]Department of Gene Therapy, University of Ulm, Helmholtzstraße 8/1, 89081 Ulm, Baden-Württemberg, Germany; [2]Department of Applied Immunology and Immunopharmacology, University Medical Center Ulm, Ulm, Germany; [3]Institute for Transfusion Medicine, University Medical Center Ulm, Ulm, Germany; [4]Institute for Clinical Transfusion Medicine and Immunogenetics Ulm, German Red Cross Blood Donation Service, Ulm, Germany; [5]Schlosspark Klinik Ludwigsburg, Privatklinik für Plastische und Ästhetische Chirurgie, Ludwigsburg, Germany; [6]Schönheitsklinik Dr. Funk, München, Germany

In adenovirus type 5 (HAdV-5)-derived viral vectors, the fiber protein has been the preferred locale for modifications to alter the natural viral tropism. Hexon, the most abundant capsid protein, has rarely been used for retargeting purposes, likely because the insertion of larger targeting peptides into Hexon often interferes with the assembly of the viral capsid. We previously observed that positively charged molecules enhance the transduction of human multipotent mesenchymal stromal cells (hMSCs)—a cell type of significant interest for clinical development but inefficiently transduced by unmodified HAdV-5-based vectors. As efficient HAdV-5-mediated gene transfer would greatly increase the therapeutic potential of hMSCs, we tested the hypothesis that introducing positively charged amino acids into Hexon might enhance the transduction of hMSCs, enabling efficient expression of selected transgenes. From the constructs that could be rescued as functional virions, one (HAdV-5-HexPos3) showed striking transduction of hMSCs with up to 500-fold increased efficiency. Evaluation of the underlying mechanism identified heparan sulfate proteoglycans (HSPGs) to be essential for virus uptake by the cells. The ease and efficiency of transduction of hMSCs with this vector will facilitate the development of genetically modified hMSCs as therapeutic vehicles in different disciplines, including oncology or regenerative medicine.

INTRODUCTION

Due to their immunomodulatory and regenerative properties, multipotent mesenchymal stromal cells (MSCs) are under clinical development as cell therapeutics. MSCs have significant therapeutic potential in several medical areas, including in regenerative medicine (e.g., wound healing or bone repair), anti-inflammatory therapy (e.g., graft-versus-host disease or inflammatory disease of the CNS), or in cancer therapy.[1–5] They can be isolated from different tissues like bone marrow,[6,7] adipose tissue, and menstrual blood, possess unique characteristics such as secretion of immunomodulatory proteins,[8,9] can differentiate into a range of cell types,[10] and autonomously migrate toward inflammatory sites and tumor tissue.[11–13] To further improve the therapeutic potential of MSCs, some of the current efforts include attempts to genetically engineer MSCs, depending on the availability of suitable procedures for efficient nucleic acid delivery into MSCs.[14]

Next to lentivirus and adeno-associated virus vectors, vectors based on human adenovirus type 5 (HAdV-5) belong to the most frequently used vector systems.[15,16] The biology of HAdV-5 is well understood, corresponding vectors are well characterized, can be easily manufactured at large scale, and have a good safety profile.[17] The versatile properties of HAdV-5 have resulted in many different applications in gene therapy,[15,18] genetic vaccination,[19,20] and oncolytic virotherapy.[21,22] Adenoviral vectors have also been used in combination with MSCs to allow the expression of therapeutic transgenes or enable MSC-mediated delivery of oncolytic viruses to tumor sites.[3–5,12,23–26] In both cases, hMSCs are isolated from a donor and genetically engineered *ex vivo* before transplantation into patients. Obviously, efficient uptake of the viral particle by MSCs is the essential first step.

As MSCs lack expression of the coxsackie and adenovirus receptor (CAR)—the primary attachment receptor of HAdV-5 particles *in vitro*—transduction of hMSCs with HAdV-5 vectors has been very inefficient.[13,25,27] As we have shown recently, one way to address this bottleneck is by using positively charged transduction enhancers to enable uptake of the negatively charged HAdV-5 vector particles into human (h)MSCs.[27] However, as transduction-enhancing agents might affect the biology of hMSCs and, importantly, their use would increase the complexity of the manufacturing process, application of genetically capsid-modified adenovirus vectors efficiently transducing hMSC would clearly be preferable. We rationally designed

Received 10 January 2022; accepted 4 March 2022;
https://doi.org/10.1016/j.omtm.2022.03.004.

Correspondence: Lea Krutzke, Ulm University, Department of Gene Therapy, Helmholtzstraße 8/1, 89081 Ulm, Baden-Württemberg, Germany.
E-mail: Lea.krutzke@uni-ulm.de

Table 1. Adenoviral vectors generated in this study

	Amino acid sequence			
Name	HVR1	HVR5	HVR7	Vector yields: (Viral particles/cell)
Wild-type: HAdV-5	DEAATALEINLEEEDDDNEDEVDEQAEQQKTHVF	EAAAGNGD	ENGWEKDATE	1.7×10^4
#1: HAdV-5-ΔHVR1	DEAATALEINL————————————QAEQQKTHVF			2.1×10^4
#2: HAdV-5-HexPos2	DEAATALEINLEEE**KKK**NE**K**EVDEQAEQQKTHVF			1.0×10^4
#3: HAdV-5-HexPos3	DEAATALEINL**KKKK**————————QAEQQKTHVF			2.6×10^4
#4: HAdV-5-HexPos4	DEAATALEINL**KKKK**————————QAEQQKTHVF	**K**AAAGNG**K**	**K**NGW**KKK**ATE	No rescue
#5: HAdV-5-HexPos5	DEAATALKINL**KK**——N**K**–V**K**-QA**K**QQKTHVF			No rescue
#6: HAdV-5-HexPos6	DEAATALKINL**KK**——N**K**–V**K**-QA**K**QQKTHVF	**K**AAAGNG**K**	**K**NGW**KKK**ATE	No rescue
#7: HAdV-5-HexPos7	DEAATALEINL**KKKKKK**——————QAEQQKTHVF			No rescue
#8: HAdV-5-HexPos8	DEAATALEINL**KKKKKKKK**———QAEQQKTHVF			No rescue
#9: HAdV-5-HexPos9	DEAATALEINL*GGSGGGSG***KKKKKKKK***GSGGGSGG*QAEQQKTHVF			No rescue

The adenoviral mutant HAdV-5 vectors generated in this study were modified in the hexon HVRs 1, 5, and 7. Sequences of HAdV-5 are based on GenBank ID: AY339865.1. The indicated amino acids (aa) correspond to the aa 136 to 170 (HVR1), 271 to 278 (HVR5), and 436 to 445 (HVR7) of the hexon protein. The negatively charged aa (underlined) were partially or entirely deleted or replaced by positively charged lysine residues (bold). The sequence of a flexible GS-linker flanking the inserted lysine residues in HAdV-5-HexPos7 is shown in italics. Rescue of vector particles was only feasible for HAdV-5-ΔHVR1, HAdV-5-HexPos2, and HAdV-5-HexPos3. Representative viral vector yields obtained by production with N52.E6 cells are listed.

HAdV-5 mutant vectors by replacing surface-exposed negatively charged amino acids (aa) with positively charged lysines. While most genetic modification approaches of adenoviruses focus on the protruding fiber protein, we altered hypervariable regions (HVRs) in the hexon protein, the most abundant adenoviral capsid surface protein and predominantly responsible for the overall net negative surface charge of the particles. Thereby we generated a set of genetically surface-charged modified HAdV-5 mutant vectors, one of which, HAdV-5-HexPos3, was found to be capable of very efficiently transducing hMSCs and also other cell types. An in-depth analysis of the underlying uptake mechanisms revealed heparin sulfate proteoglycans (HSPGs) to be essential for the improved and CAR-independent transduction abilities of HAdV-5-HexPos3.

RESULTS

Generation of charge-modified HAdV-5 mutant vectors

It was previously shown that the deletion of a negatively charged 13-aa loop (EEEDDDNEDEVDE) within HVR1 of HAdV-5 Hexon is tolerated.[28] Based on these data, we generated several Hexon-modified adenoviral mutant vectors. Negatively charged aa within HVR1, HVR5, and HVR7 were deleted and partially replaced by positively charged lysine residues (Table 1). Strikingly, from nine constructs, only three could be rescued as functional viral vectors, suggesting detrimental effects on particle formation by the alterations introduced. HAdV-5-ΔHVR1 is similar to a vector generated by Alemany et al.,[28] in HAdV-5-HexPos2 four aspartic acid residues within the 13-aa loop were replaced by lysines, and in HAdV-5-HexPos3 four consecutive lysines replaced the 13-aa loop. The three mutant vectors could be produced in N52.E6 cells with high viral vector yields of 1 to 5×10^4 particles/cell, which is comparable to yields routinely obtained with wild-type capsid HAdV-5 vectors (Table 1). Genetic modifications were confirmed by sequencing and restriction analysis (data not shown). At the protein level, SDS-PAGE with subsequent silver staining of denatured viral particles confirmed an influence of these modifications on the running behavior of Hexon (Figure 1A). Moreover, we determined the viral surface charge by zeta potential measurements (Figure 1B). Compared with HAdV-5 (−22.8 ± 2.8 mV), all the mutants, in particular HAdV-5-HexPos3 (−8.1 ± 0.4 mV), but also HAdV-5-HexPos2 (−17.3 ± 1.3 mV) and HAdV-5-ΔHVR1 (−19.4 ± 2.2 mV), showed significant reduction of the net negative surface charge.

Human MSCs are efficiently transduced with HAdV-5-HexPos3

Human MSCs (hMSCs) naturally migrate toward inflammation and tumor sites.[29] Therefore, they represent attractive carrier cells for the transport of oncolytic adenoviruses or vector-encoded therapeutic proteins to respective locations.[2,30] However, due to the lack of CAR expression, hMSCs are very difficult to transduce with HAdV-5 vectors. As we previously observed that positively charged molecules significantly enhanced HAdV-5-mediated gene transfer into hMSCs,[27] we analyzed transduction of bone marrow-derived (BM-) and adipose tissue-derived (A-) hMSCs with the charge-modified vectors HAdV-5-ΔHVR1, HAdV-5-HexPos2, and HAdV-5-HexPos3. We observed a striking 500-fold increase in mean fluorescence intensity (MFI) of BM-hMSCs after transduction with HAdV-5-HexPos3 compared with HAdV-5 (Figure 2A). Similar results were obtained for the transduction of A-hMSCs, for which an up to 175-fold increased MFI was detected for HAdV-5-HexPos3-compared with HAdV-5-transduced cells (Figure 2B). HAdV-5-ΔCAR-HexPos3 vector particles, ablated for CAR-binding due to a point mutation in the fiber knob,[31] transduced hMSCs with the same efficiency as their CAR-binding counterparts, which confirmed a CAR-independent transduction mechanism. Interestingly, vectors carrying the ΔHVR1 or HexPos2 mutations showed no effects on transduction efficiencies for both BM-hMSCs and A-hMSCs. These results are further supported by the proportion of EGFP-expressing cells. With

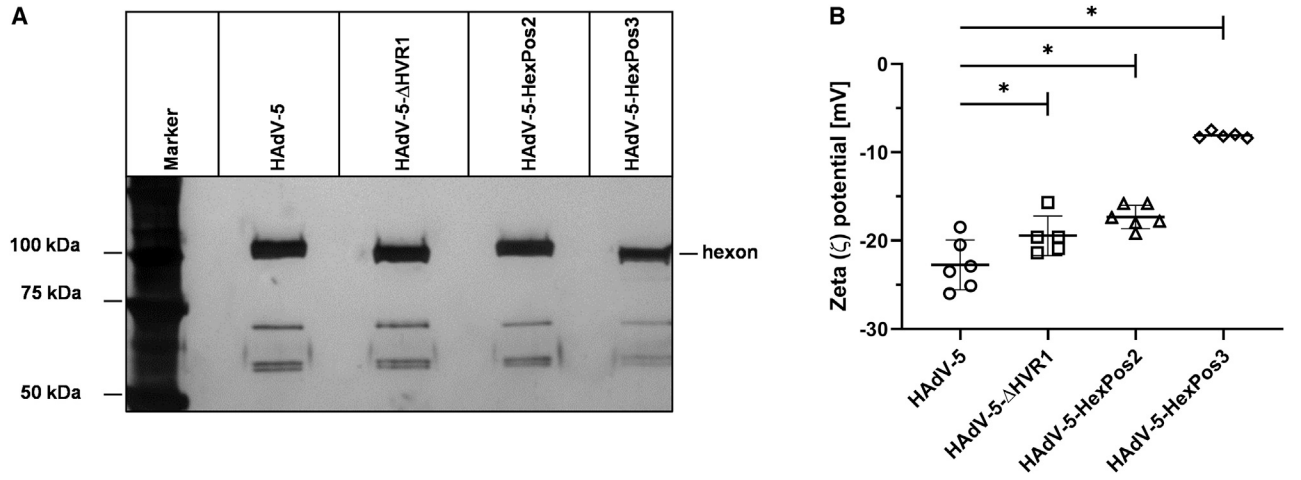

Figure 1. Genetic modification of HAdV-5 in hexon HVR1 influences the running behavior of hexon and reduces the negative surface charge of adenoviral particles

(A) Silver staining of 5×10^9 denatured adenoviral particles separated by reducing SDS-PAGE. (B) The surface charge of the indicated dialyzed adenoviral vectors was analyzed using zeta potential measurements. Results are given as mean ± SD. Ordinary one-way ANOVA with subsequent Dunnett's multiple comparison was used for statistical analysis. *$p \leq 0.05$.

physical multiplicity of infection (pMOIs) of 1,000, only 2% to 5% of BM-hMSCs were transduced with HAdV-5, HAdV-ΔHVR1, and HAdV-HexPos2 (Figure S1A). However, vectors carrying the HexPos3 mutation enabled transduction of up to 80% of BM-MSCs. Similar results can be reported for A-hMSCs: transduction with HAdV-5, HAdV-ΔHVR1, and HAdV-HexPos2 resulted in <5% EGFP-positive cells, whereas transduction with HAdV-5-HexPos3 or HAdV-5-ΔCAR-HexPos3 resulted in about 50% EGFP-positive cells (Figure S1B). The significantly enhanced transduction efficiency becomes furthermore visible in fluorescence microscopy images, where EGFP expression is impressively enhanced in cells transduced with HAdV-5-HexPos3 (Figure 2C).

Efficient CAR-independent transduction of tumor cells with HAdV5-HexPos3

As HAdV-5-HexPos3 showed enhanced transduction of hMSCs, we analyzed whether the Hexon modification also influenced the transduction of other potential target cells. In MSC-based oncolytic virotherapy, hMSCs are used as carrier cells for oncolytic adenoviruses to enable efficient local delivery of the oncolytic viruses to the tumor after systemic administration. Thus, not only efficient transduction of the hMSCs is essential for the therapeutic efficacy, but also efficient transduction of the targeted tumor cell. Therefore, we performed *in vitro* transduction assays of the tumor cell lines UM-SCC-11B (head and neck squamous cell carcinoma), MiaPaCa (pancreatic carcinoma), Huh7 (hepatocellular carcinoma), HepG2 (hepatocellular carcinoma), and A549 (lung adenocarcinoma) (Figure 3A). In addition to the EGFP-expressing HAdV-5 and HAdV-5-HexPos3 vectors, the transduction assay was performed with the corresponding ΔCAR vectors (HAdV-5-ΔCAR and HAdV-5-ΔCAR-HexPos3). HAdV-5-HexPos3 showed transduction efficiencies similar to unmodified HAdV-5 for MiaPaCa, Huh7, and A549 cells; however, noticeably improved transduction of UM-SCC-11B and HepG2 cells. Interestingly, significantly enhanced cell transduction was observed for CAR-binding ablated HAdV-5-ΔCAR-HexPos3 vectors relative to the HAdV-5-ΔCAR counterparts. The increase in transduction with the HexPos3 mutant was particularly strong for UM-SCC-11B (>16-fold) and MiaPaCa (>33-fold) cells. Nevertheless, enhanced, although less distinct, transduction with HAdV-5-ΔCAR-HexPos3 was also observed for A549, Huh7, and HepG2 cells.

Viral replication is preserved for HAdV-5-HexPos3

For the utilization of a vector in oncolytic therapy, not only target cell infection is essential but also efficient viral replication and release of viral progeny. To analyze viral amplification of the HexPos3 mutant vector, we infected the *E1*-complementing cell line HEK293T with HAdV-5-ΔCAR and HAdV-5-ΔCAR-HexPos3 vectors at low pMOIs to allow for several replication cycles. On day 6 after infection, plates were washed to remove cells that detached upon adenoviral replication. The remaining cells were stained using crystal violet. Subsequently, crystal violet was quantified by OD_{560nm} measurements after methanol extraction. Low OD_{560nm} values correspond to a low amount of remaining cells and indicate efficient adenoviral replication and virus-mediated cell lysis, whereas higher OD_{560nm} values refer to high numbers of remaining cells. Results revealed that neither replication nor cell lysis by HAdV-5-ΔCAR-HexPos3 was impaired compared with HAdV-5-ΔCAR but rather slightly improved (Figure 3B).

The HexPos3 mutation does not significantly alter relevant interactions with non-cellular blood components

In combination with oncolytic HAdV-5 vectors, hMSCs are used to enable systemic delivery of oncolytic particles to the tumor site, bypassing the extensive sequestration of HAdV-5 particles. Although

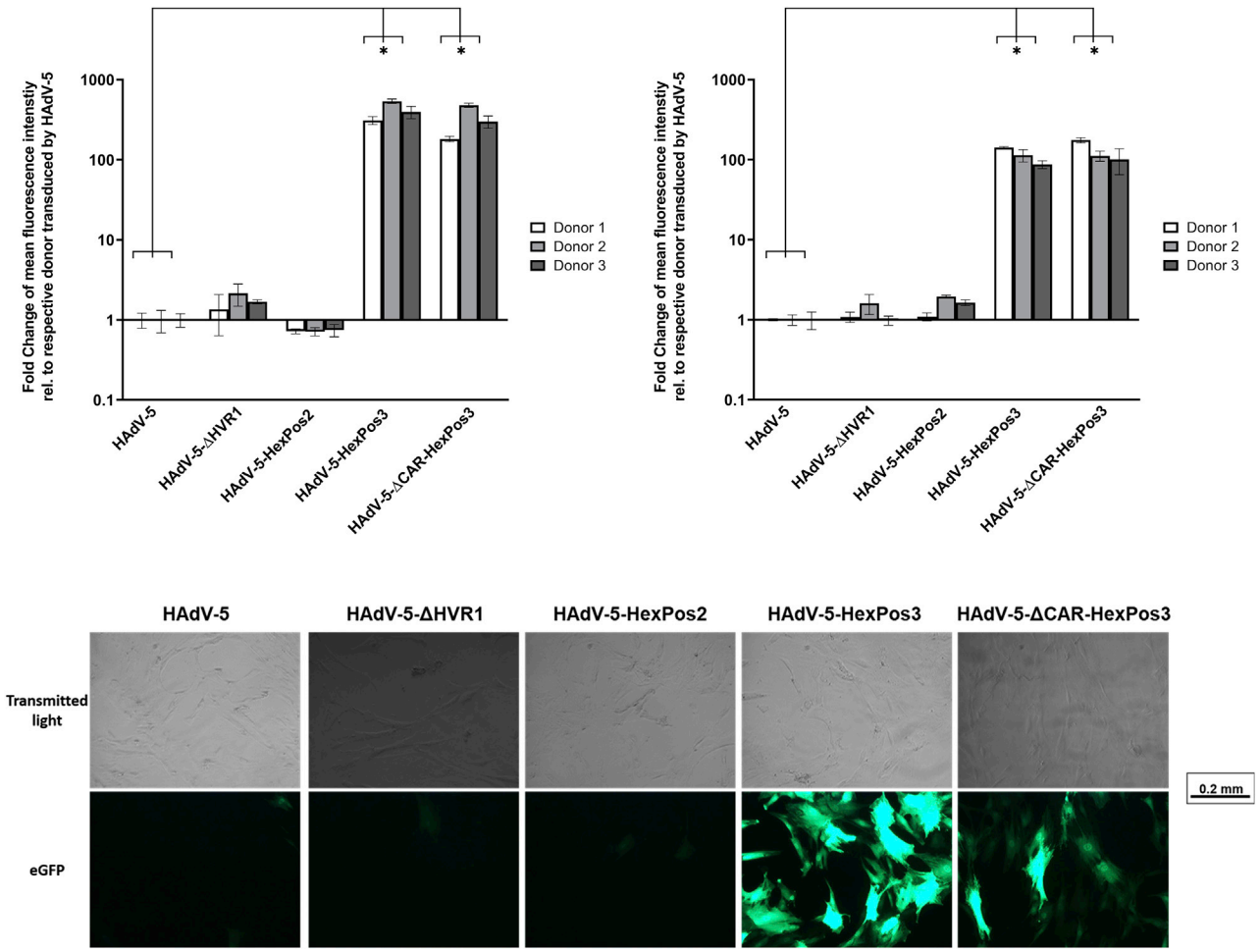

Figure 2. Enhanced transduction of hMSCs by HAdV-5-HexPos3

An amount of 3×10^4 BM-hMSCs (A) or A-hMSCs (B) were transduced with the indicated adenoviral vectors using a pMOI 1,000. Twenty-four hours p.t., EGFP expression was analyzed by flow cytometry. The results of three different MSC donors (biological triplicates each) are shown as mean ± SD. One-way ANOVA with subsequent Tukey's multiple comparison was used for statistical analysis. *$p \leq 0.05$ (C) Microscopic images (brightfield and fluorescence) of EGFP expression in BM-hMSCs transduced with the indicated adenoviral vectors using pMOI 1,000, 24 h p.t.

hMSCs protect viral particles from sequestration during transport, particles come into contact with cellular and non-cellular blood components once the cells become lysed and viral progeny are released, resulting in non-target interactions at the highly vascularized tumor site. In the context of these interactions, the adenoviral hexon protein plays an important role. For example, blood coagulation factor X (FX), known to bind to HVR5 and HVR7 of the hexon protein, mediates uptake of viral particles by hepatocytes.[32–35] Moreover, most neutralizing immunoglobulin (Ig)G antibodies are directed to Hexon,[36,37] and it has been shown that natural IgMs bind to the negatively charged residues within HVR1 of the hexon protein.[38–40] Therefore, we analyzed if the here-described Hexon modifications interfered with these interactions.

First, we analyzed whether HAdV-5-HexPos3 was neutralized by IgG antibodies. HAdV-5 and HAdV-5-HexPos3 particles were pre-incubated with different amounts of a neutralizing antibody targeting Hexon, which was followed by transduction of A549 cells. These experiments revealed that the Hexon modification of HAdV-5-HexPos3 did not influence IgG-mediated neutralization, as both vectors were neutralized with equal efficiency in an IgG concentration-dependent manner (Figure 4A).

In order to investigate whether putative conformational changes resulting from the alterations within HVR1 altered the binding of FX, we performed surface plasmon resonance (SPR) measurements, comparing HAdV-5 with HAdV-5-ΔHVR1 and HAdV-5-HexPos3. To analyze whether one of the introduced mutations in HVR1 mediated binding to FX, we additionally generated FX binding-ablated vector variants (referred to as Δ5FX), which harbor five point mutations in HVR5 and HVR7, as described by Atasheva et al.[39] Compared with unmodified HAdV-5 vectors, both HAdV-5-ΔHVR1 and

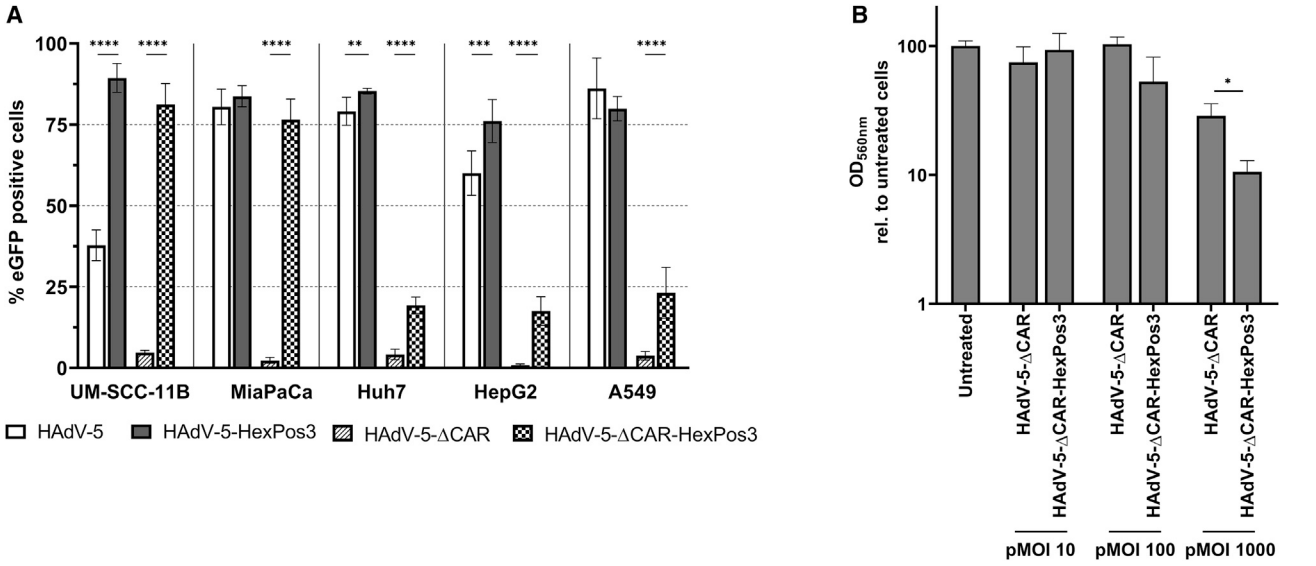

Figure 3. Transduction of various tumor cell lines and maintained replication efficiency of HAdV-5-HexPos3

(A) Cells were transduced with a pMOI 1,000 of the indicated adenoviral vectors and analyzed for EGFP expression 24 h p.t. by flow cytometry. Results are shown as mean ± SD. Student's t test with Welch's correction was used for statistical analysis. (B) An amount of 5×10^4 HEK293T cells were infected with the indicated pMOIs of the respective adenoviral vectors. Six days p.i., the remaining cells were stained with crystal violet. Crystal violet was extracted with methanol, and the optical density at 560 nm was determined. Representative results of one out of three experiments are given as mean ± SD. Student's t test was used for statistical analysis. *$p \leq 0.05$.

HAdV-5-HexPos3 showed slightly increased binding to FX (relative response units normalized to HAdV-5 in Figure 4B, absolute response signals in Figure S2), indicating that the charge modification of Hexon might result in enhanced binding of FX to the adenoviral capsid. All FX binding-ablated (Δ5FX) counterpart vectors did not show any FX binding, indicating that the introduced HVR1 mutations themselves did not facilitate FX binding.

Binding of FX to the generated vectors was additionally verified by transduction of CAR-negative SKOV-3 cells in the presence or absence of physiological concentrations of human FX.[41] Transduction efficiencies were relatively low in the absence of FX; however, transduction with HAdV-5 or HAdV-5-HexPos3 was significantly enhanced in the presence of FX (Figures 4C and S3). This assay also confirmed the expected lack of FX binding to the Δ5FX vector variants, as no transduction-enhancing effect of FX was observed. Taken together, both biophysical analysis of FX binding to Hexon by SPR measurements and biological assays analyzing FX-mediated SKOV-3 transduction confirmed that FX binding to HAdV-5-HexPos3 was not inhibited.

Unexpectedly, in the absence of FX, HAdV-5-HexPos3-Δ5FX showed enhanced transduction of SKOV-3 cells compared with HAdV-5-HexPos3, and similar results were with several tumor cell lines (Figure S4A). As the introduced Δ5FX mutation encompassed the replacement of two negatively charged glutamic acids by neutrally charged aa residues (E424S, E451Q), we hypothesized that a further reduction of the net negative surface charge caused the improvement in transduction. In fact, zeta potential analysis confirmed that HAdV-5-Δ5FX-HexPos3 (−3.71 ± 0.06 mV) was less negatively charged than HAdV-5-HexPos3 (−4.89 ± 0.36 mV) (Figure S4B). We also analyzed transduction of BM- and A-hMSCs with Δ5FX-carrying vectors; however, in these cell types, the introduced point mutations did not affect transduction (data not shown).

While the improved tumor cell transduction by Δ5FX-carrying vectors could be beneficial for oncolytic approaches, the absence of FX binding was shown to result in efficient neutralization of HAdV-5 particles by natural IgMs.[42] Atasheva et al.[39] recently revealed that the negative charge of HVR1 of Hexon is highly relevant for binding of natural IgMs to HAdV-5 particles, as HVR1-deleted vectors were protected from natural IgM-mediated neutralization despite ablated FX binding. Therefore, we hypothesized that HAdV-5-Δ5FX-HexPos3 with ablated FX binding might additionally be protected from IgM-mediated neutralization, as in this vector positively charged lysines almost completely replace the negatively charged HVR1. Both the FX-binding and FX-binding ablated vector variants were applied in an *in vitro* neutralization assay using complement-preserved HAdV-5-naïve human plasma as a source of natural IgMs (Figure 4D). Vectors were pre-incubated with human plasma, which was followed by transduction of A549 cells. As expected, HAdV-5 and HAdV-5-HexPos3 particles were not neutralized, likely due to the binding of FX present in plasma. Unexpectedly, not only HAdV-5-Δ5FX but also HAdV-5-Δ5FX-HVR1 and HAdV-5-Δ5FX-HexPos3 vectors were efficiently neutralized in HAdV-5-naïve plasma, indicating that neither the insertion of lysine residues nor the deletion of the 13-aa stretch in the HVR1 loop were sufficient to prevent binding of natural IgMs. Since HAdV-5-HexPos3 particles are

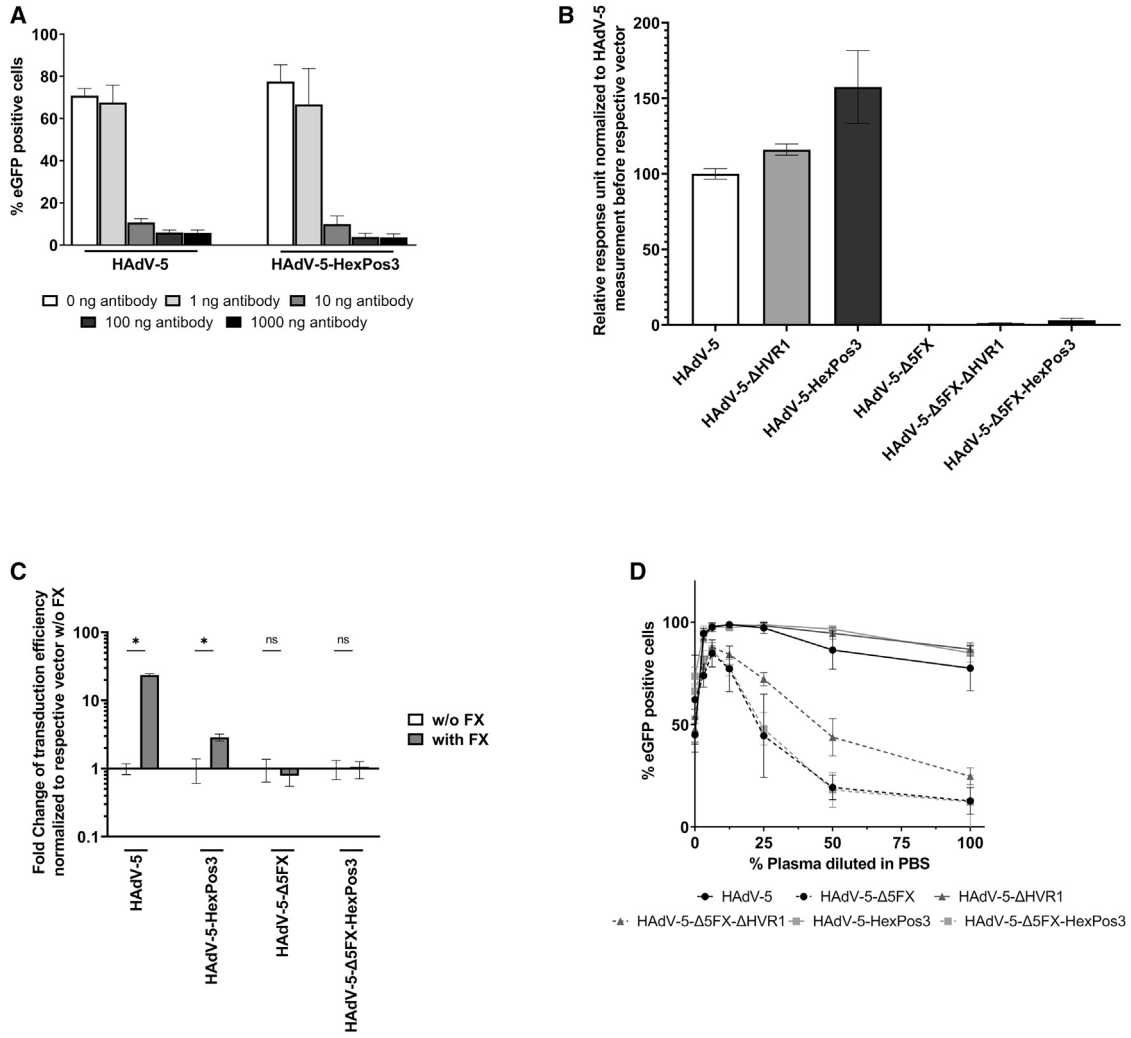

Figure 4. HAdV-5-HexPos3 binds to blood coagulation FX and is neutralized by hexon-specific IgGs as well as HAdV-5-naïve blood components

(A) HAdV-5 or HAdV-5-HexPos3 particles were incubated with the indicated amount of an α-hexon IgG before transduction of A549 cells. Twenty-four hours p.t., EGFP expression was analyzed by flow cytometry. (B) Analysis of vector binding to immobilized FX by SPR. Unmodified HAdV-5 particles were measured prior to each vector of interest. Relative response units (normalized to the respective HAdV-5 measurement) are shown as mean ± SD. (C) SKOV-3 cells were transduced with pMOI 1,000 in the absence or presence of physiological human FX concentrations (8 μg/mL). Seventy-two hours p.t., EGFP expression was analyzed by flow cytometry. Results are shown as fold change ±SD in transduction efficiency, normalized to the respective vector without FX. Statistical analysis was performed using the Student's t test. *$p \leq 0.05$. See also Figure S2. (D) The indicated viral particles were incubated with different dilutions of HAdV-5-naïve plasma before transduction of A549 cells. Twenty-four hours p.t., EGFP expression was analyzed by flow cytometry.

efficiently neutralized by natural IgMs, we assume that Δ5FX-carrying vectors are disadvantageous for oncolytic approaches despite the improved tumor cell transduction, as FX-shielding from attack by natural IgMs might be of high relevance.

HAdV-5-HexPos3 is superior for transduction of hMSCs compared with HAdV-5/3

Since HAdV-5-HexPos3 very efficiently transduced hMSCs, we compared it with HAdV-5/3 vectors—a chimeric HAdV-5-based vector that carries the fiber knob of HAdV-3 and was previously described to transduce hMSCs very efficiently.[43] Transduction of BM-hMSCs and A-hMSCs showed that HAdV-5/3 vectors increased transduction efficiency of both cell types compared with unmodified HAdV-5 vectors (Figures 5A, 5B, S5B, and S5C). Strikingly, of the tested vectors, HAdV-5-HexPos3 turned out to be the most efficient adenoviral vector. For the transduction of BM-hMSCs and A-hMSCs, HAdV-5-HexPos3 achieved transduction efficiencies of >80%, compared with <10% (BM-hMSCs) and <35% (A-hMSCs) for HAdV-5/3 vectors. A combination of the chimeric fiber protein and the HexPos3 mutations did not further improve the transduction of hMSCs. To confirm vector integrity of the chimeric HAdV-5/3, we analyzed the transduction of various tumor cell lines with HAdV-5/3

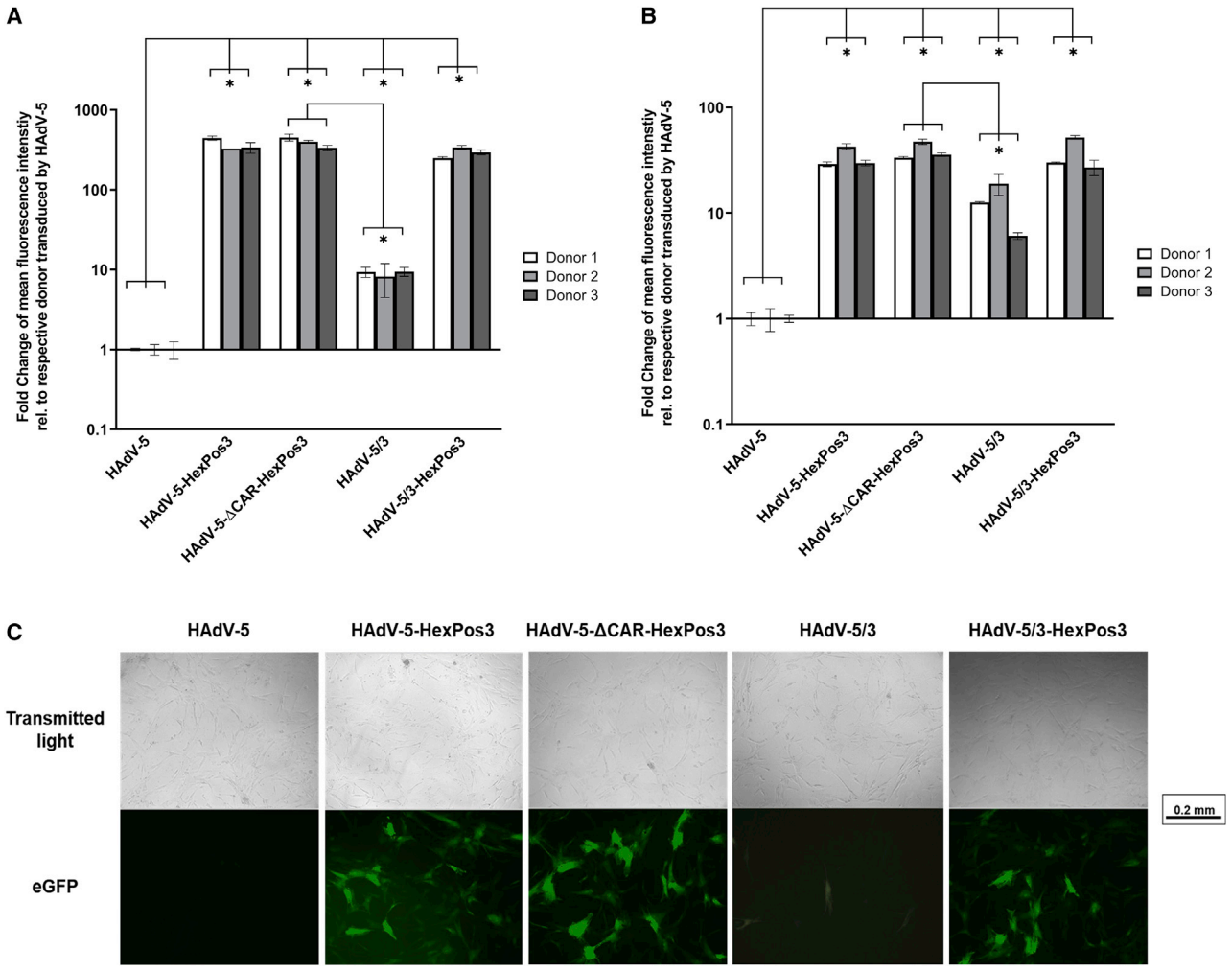

Figure 5. HAdV-5-HexPos3 outperforms HAdV-5/3 regarding transduction of hMSCs

BM-hMSCs (A) or A-hMSCs (B) were transduced with the indicated adenoviral vectors using pMOI 1,000. Twenty-four hours p.t., EGFP expression was analyzed by flow cytometry. Results of three different MSC donors (biological triplicates each) are shown as mean ± SD. One-way ANOVA with subsequent Tukey's multiple comparison was used for statistical analysis. *$p \leq 0.05$. (C) Microscopic images (brightfield and fluorescence) of EGFP expression in BM-hMSCs transduced with the indicated adenoviral vectors with pMOI 1,000 24 h p.t.

and HAdV-5/3-HexPos3 vectors (Figure S6). Vector integrity was confirmed, as both vectors showed very efficient, though cell type-dependent, transduction.

HSPGs are essential for HAdV-5-HexPos3-mediated cell transduction in a CAR-independent manner

Transduction experiments of various cancer cell lines and hMSCs demonstrated that HAdV-5-HexPos3 is an efficient gene delivery tool irrespective of cell surface CAR expression levels. Heparan sulfate proteoglycans (HSPGs) are used for cell attachment by various viruses, including adeno-associated virus (AAV) type 2 and 3b,[44,45] or respiratory syncytial virus.[46] Moreover, it is known that FX-mediated HAdV-5 cell transduction (e.g., SKOV-3 transduction, Figure 4C) is dependent on cell surface HSPGs. Since HSPGs are predominately bound by positively charged molecules,[44] we analyzed if enhanced transduction of HAdV-5-HexPos3 vectors might be mediated by the binding of the particles to cell surface HSPGs. HAdV-5-HexPos3 and HAdV-5-ΔCAR-HexPos3 were incubated with increasing amounts of the HSPG-analog heparin and transduction of CAR-expressing UM-SCC-11B cells was analyzed (Figure 6A). A concentration-dependent decrease in transduction was observed for both vectors. At the highest heparin concentration, cell transduction with HAdV-5-HexPos3 and HAdV-5-ΔCAR-HexPos3 was decreased by 68.0% ± 4.0% and 92.8% ± 1.1%, respectively. This indicated that heparin bound to the HexPos3 capsid and subsequently inhibited attachment to target cells. As HAdV-5-HexPos3 retained some infectivity and HAdV-5 transduction was not inhibited by heparin (data not shown), the interaction

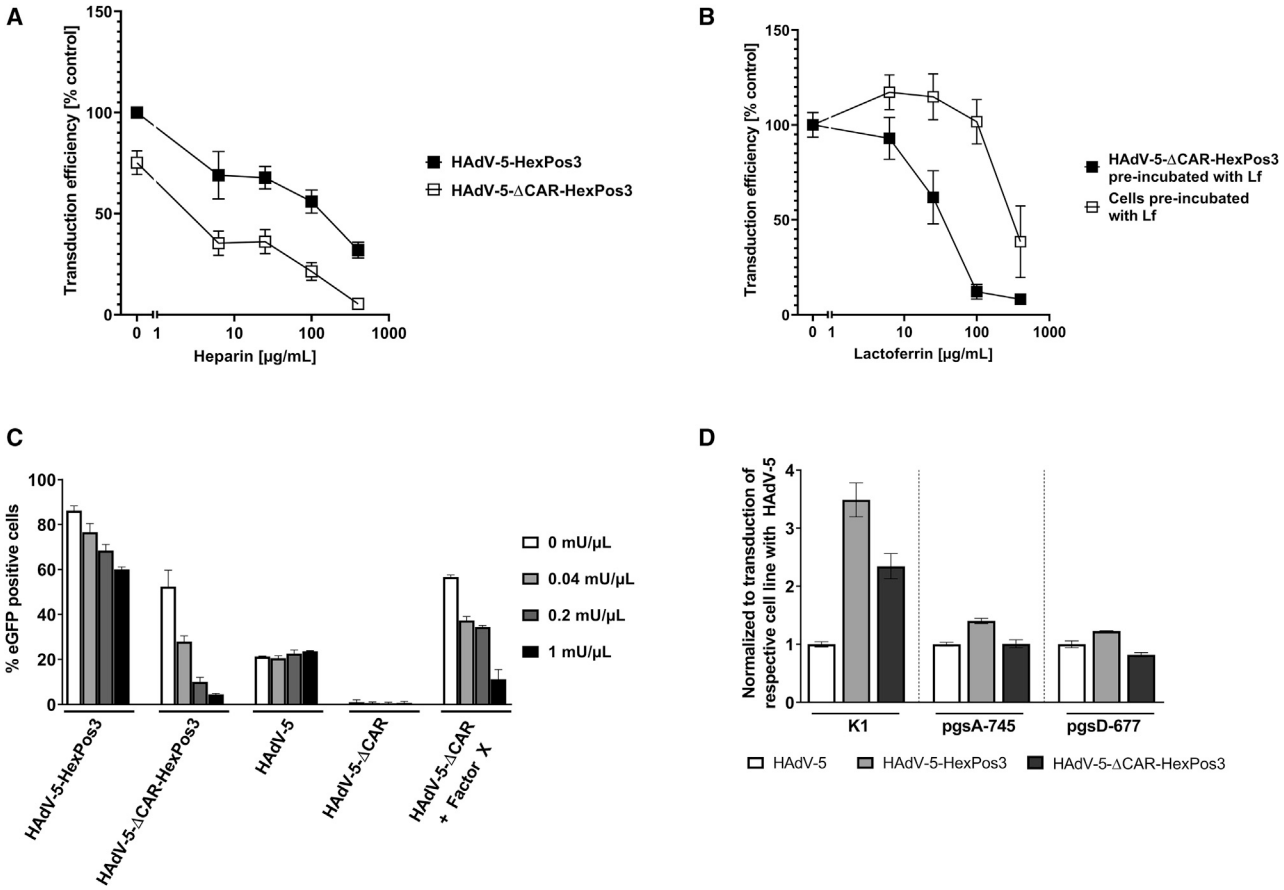

Figure 6. Cell surface HSPGs are essential for CAR-independent HAdV-5-HexPos3 cell transduction

(A) Vector particles were pre-incubated with the indicated amounts of heparin in serum-free medium at 37°C before being used for transduction of UM-SCC-11B cells with a pMOI 1,000. Twenty-four hours p.t., cells were analyzed for EGFP expression by flow cytometry. Results are given as mean ± SD of transduction relative to the transduction efficiency of HAdV-5-M3 without heparin. (B) UM-SCC-11B cells or HAdV-5-M3-ΔCAR particles were pre-incubated with the respective amounts of lactoferrin (Lf) in serum-free medium at 37°C before transduction of cells with a pMOI 1,000. EGFP expression was analyzed by flow cytometry 24 h p.t. Results are given as mean ± SD of transduction relative to the transduction efficiency of the respective vector without Lf. (C) UM-SCC-11B cells were treated with the indicated amounts of heparinase I for 1 h before transduction of cells with a pMOI 1,000. EGFP expression was analyzed 24 h p.t. by flow cytometry. (D) CHO K1, CHO pgsA-745, and CHO pgsD-677 cells were transduced with the indicated adenoviral vectors with pMOI 2000. Flow cytometric analysis of EGFP expression was performed 24 h p.t.

of heparin with the viral capsid appeared to not impede the CAR-dependent transduction mechanism.

To further confirm these results, we performed additional transduction-inhibition assays using human lactoferrin (Lf). Lf, a component of the non-specific immune system, exerts its distinct antiviral roperties by blocking heparan sulfate moieties on the cell surface.[47] To analyze if Lf inhibited cell transduction of HexPos3-carrying vectors, transduction of UM-SCC-11B cells was performed after pre-incubation of viral particles with Lf (Figure 6B). In line with the heparin transduction experiments, we observed a significant decrease in transduction efficiency for HexPos3 vectors by up to 91.9% ± 2.8% with increasing amounts of Lf. To further investigate whether Lf inhibited cell transduction by binding to the viral capsid or to the cell surface, we pre-incubated UM-SCC-11B cells with Lf. Before the vector was added, cells were thoroughly washed and fresh medium was added. Results showed a reduction of transduction efficiency by 61.5% ± 18.8%, suggesting that Lf exerted its inhibitory effect at least in part via binding to the cell surface. Moreover, these data suggested that Lf and the HexPos3 vector competed for similar moieties on the cell surface, most likely HSPGs. It is noteworthy that transduction of cells by HAdV-5 was not significantly altered by the different pre-incubation settings (data not shown).

To analyze whether enzymatic removal of HSPGs on the cell surface inhibited transduction with HAdV-5-HexPos3, UM-SCC-11B cells were treated with heparinase I or II prior to transduction. Results revealed that treatment with both, heparinase I and II, respectively, completely inhibited HAdV-5-ΔCAR-HexPos-3-mediated cell transduction, whereas transduction with CAR-binding vectors was not substantially inhibited, confirming that HSPGs on the cell surface

were essential for efficient HexPos3-mediated cell transduction (Figures 6C and S7).

To verify this observation, we transduced the HSPG-deficient Chinese hamster ovary (CHO) cell lines pgsA-745 and pgsD-677, as well as the HSPG-expressing CHO K1 cells, with the different adenoviral vectors. Transduction of CHO K1 cells with HAdV-5 resulted in ~10% EGFP-positive cells, which was increased to ~32% with HAdV-5-HexPos3 (Figure 6D). This transduction-enhancing effect of the HexPos3 mutation was not observed with HSPG-negative CHO pgsA-745 and CHO pgsD-677 cells.

Taken together, experiments using heparin, lactoferrin, heparinases, and HSPG-deficient CHO cell lines revealed that HSPGs play an essential role in the HexPos3-mediated adenoviral vector uptake mechanism.

DISCUSSION

Human MSCs are under preclinical and clinical development for many different applications. The genetic modification may be a way to further increase their therapeutic potential and promote clinical translation: cell surface modification can enhance migration of hMSCs,[48,49] transgene expression may influence their immunomodulatory functions,[50,51] and hMSCs can also be used as carriers for the transport of oncolytic viruses to tumors.[5] All these approaches rely on an efficient gene delivery into this cell type. Different strategies to genetically modify MSCs have been pursued with lentiviral or AAV vectors.[52,53] Lentiviral vectors enable stable expression of encoded proteins.[54] However, chromosomal integration also harbors the risk of insertional mutagenesis.[55] Since MSC-based treatments are predominately temporary therapies, long-term gene expression is generally not required. The cargo capacity of lentiviral vectors is up to about 10 kb, while for AAV vectors the cargo limit is smaller at 5 kb.[56–58] Adenoviral vectors do not integrate chromosomally and, depending on the vector used, can accommodate up to ~2.5 kb (wild-type virus), ~8 kb (first generation vectors) or ~36 kb (gutless vectors) of foreign DNA.[59,60] However, *ex vivo* transduction of hMSCs with HAdV-5-based vectors is very inefficient due to a lack of CAR expression on this cell type.[13,27] We recently identified several transduction enhancers that can be used to enhance HAdV-5-mediated gene transfer into hMSCs.[27] However, while transduction enhancers are a readily available adjuvant for *in vitro* transduction experiments, prior to clinical use, a potential impact on the biology and functionality would need to be considered. In addition, using transduction enhancers as part of a production process under good manufacturing process conditions would increase process complexity, potentially negatively affect scalability and reproducibility, and significantly increase overall costs. Thus, the generation of a genetically modified HAdV-5 vector for more efficient hMSC transduction would be attractive. Since most of the identified transduction enhancers shared a positive charge as a common factor, we tested the hypothesis that the insertion of positively charged aa residues into surface-exposed regions of the adenoviral capsid might improve transduction of hMSCs.

While most genetic modifications of the adenoviral capsid focus on the protruding fiber protein, we altered distinct surface-exposed aa in the hexon protein, with 720 copies per particle the most abundant protein in the viral capsid compared with 36 copies of fiber protein.[61] We generated several adenoviral mutant vector constructs with modifications in HVR1, HVR5, and HVR7 with the aim to remove negatively charged aa residues and partially replace them with positively charged lysines. However, most of the DNA constructs could not be rescued as functional virions, probably because the modifications interfered with proper Hexon folding, trimerization, or with capsid assembly. However, three of nine mutants could be produced, all modified in HVR1. HVR1 presents a loop of 32 aa that harbors a stretch of 13 negatively charged aa conferring most of the negative charge to the outer capsid surface.[62] Our zeta potential measurements showed that all HVR1-modified vectors had a reduced net negative surface charge. Functionally, use of HAdV-5-HexPos3, having the least negative net surface charge, resulted in dramatically improved transduction of BM-hMSCs and of A-hMSCs that even surpassed the chimeric HAdV-5/3 vector that previously had been found useful for transduction of hMSCs.[43] The high transduction efficiency of the HAdV-5-HexPos3 capsid, together with the large cargo capacity of adenoviral vectors, could pave the way for improved MSC-based therapies. For example, the migration behavior of MSCs can be improved by overexpression of specific surface receptors,[48] while the immunomodulatory capabilities of MSCs can be enhanced by the expression of therapeutic proteins.[50] Due to the up to 36-kb cargo capacity of HAdV-5 vectors, multiple transgenes could be expressed at the same time, thereby addressing several bottlenecks of MSC-based therapies at once.

In addition, HAdV-5-HexPos3 particles showed improved transduction of several tumor cell lines and maintained viral replication, suggesting that HexPos3 vectors could be promising candidates for MSC-based oncolytic virotherapy. Making use of their natural migration toward inflammation sites, hMSCs are being evaluated as carrier cells for delivery of oncolytic viruses to the tumor site, thereby enabling systemic administration of oncolytic adenoviruses while bypassing extensive particle sequestration. Once the carrier cells are lysed, viral progeny are released in direct vicinity to the targeted tumor cells. However, as the tumor microenvironment is highly perfused, the interaction with cellular and non-cellular blood components constitutes another barrier. Here, the binding of HAdV-5 to human erythrocytes is an important factor: as erythrocytes possess CAR on their surface, HAdV-5 binds to human erythrocytes with high affinity, representing one of the major sinks of administered HAdV-5 particles.[63,64] In this study, we showed that HAdV-5-HexPos3 enabled efficient transduction of target cells in a CAR-independent manner highlighting its potential for oncolytic approaches exploiting carrier cells, such as hMSCs, as CAR-binding ablated HAdV-5 vectors can be used, avoiding the binding of progeny particles to erythrocytes.

Besides binding to erythrocytes, adenoviral particles may be neutralized by natural IgMs in the well-perfused tumor microenvironment. It has been shown that the negatively charged HVR1 is a target region

for the binding of natural IgMs to the HAdV-5 capsid.[39] Thus, we hypothesized that HAdV-5-HexPos3 particles might escape from natural IgM-mediated neutralization. Unexpectedly, the deletion of 13 negatively charged aa in HVR1 did not prevent the neutralization of particles in HAdV-5-naïve plasma. This strongly indicated the binding of natural IgMs to the modified hexon proteins, indicating that different from the Hexon modification presented by Atasheva et al.,[39] the here-introduced modifications are not sufficient to protect from natural IgM-mediated neutralization. However, a study by Xu et al. revealed that human FX shields HAdV-5 particles from attack by natural IgMs and complement.[42] Here, we evaluated the interaction of HexPos3-particles with human FX and showed that the inserted mutation of HAdV-5-HexPos3 did not inhibit FX binding. Thus, the FX-mediated protection of HAdV-5-HexPos3 particles from natural IgM and complement neutralization is maintained.

Interestingly, SPR analysis revealed slightly improved binding of human FX to the HAdV-5-HexPos3 particles. It is unlikely that the positively charged lysines introduced in Hexon HVR1 form an additional binding site for FX, since HAdV-5-Δ5FX-HexPos3 particles did not exhibit any FX binding. Instead, in wild-type HAdV-5 Hexon protein, the negatively charged HVR1 might interfere with the binding of FX to the hexon protein; hence, binding was improved upon deletion of the 13 negatively charged aa stretch. This observation is in line with the findings of Sumarheni et al.,[65] who constructed an FX GLA domain-derived 40-mer polypeptide, which surprisingly was found to bind to HVR1. Strikingly, an increased affinity of FX to the hexon protein was detected in the presence of the 40-mer polypeptide. The authors concluded that upon binding of the polypeptide, a polypeptide-induced rigidification or folding of the HVR1 loop might offer better access of the hexon protein to FX. Taking our observations and the observations of Sumarheni et al.[65] together, this might indicate that the intrinsically disordered HVR1 loop of wild-type HAdV-5 might negatively influence the binding of FX to the hexon trimer.

As our transduction experiments revealed that HAdV-5-HexPos3 mediated a Hexon-dependent particle uptake into target cells independent of cell surface CAR expression, the typical primary attachment receptor of HAdV-5 vectors, we were interested in identifying a possible attachment receptor for HexPos3 particles.[66,67] Our results indicate that HSPGs are essential for HAdV-5-HexPos3-mediated cell uptake. It is well-known that positively charged aa residues interact with HSPGs. For example, a cluster of four consecutive positively charged arginine residues in the Lf protein (G**RRRR**S) has been found to be involved in the interaction with HSPGs.[47] From a biochemical point of view, this motif shares distinct similarities with the sequence of the mutated Hexon HVR1 of HAdV-5-HexPos3, which also carries four consecutive positively charged lysine residues (L**KKKK**Q). Also in the capsids of AAV types 3b and 2, arginine and lysine residues are considered as relevant for HSPG-mediated attachment to target cells.[44,45,68] It has also been shown that insertion of lysine residues into the fiber knob domain of HAdV-5 vectors resulted in HSPG targeting.[69] It is known that the negatively charged sulfate and carboxyl groups of HSPGs mediate binding to positively charged arginine and lysine residues.[70,71] This supports our assumption that interaction with cell surface HSPGs is crucial in the CAR-independent transduction mechanism of HAdV-5-HexPos3. As previously shown, FX binds to HAdV-5 Hexon,[72] and subsequently mediates hepatocyte transduction. HAdV-5:FX complexes interact with HSPGs on the cell surface,[73] and the hepatic uptake of these complexes is highly dependent on heparan sulfate sidechain sulfation, with particular importance of *O*-sulfation.[74] Interestingly, our data show that SKOV-3 cells were efficiently transduced by HAdV-5:FX complexes but not by HAdV-5-HexPos3. Therefore, we assume that the HSPG-binding mechanism of HAdV-5-HexPos3 likely differs from that of vector-bound FX.

Taken together, we here describe design, generation, and biophysical and functional characterization of a charge-modified HAdV-5-based vector that allows very efficient transduction of BM- and A-hMSCs HSPG-dependently, expanding the therapeutic potential of hMSCs, for example, by expression of therapeutic proteins or as a carrier for oncolytic adenoviruses.

MATERIALS AND METHODS

Cell culture

All cells were cultivated at 90% humidity, 5% CO_2, and 37°C and passaged twice a week. Cells were detached with 0.05% trypsin-EDTA (Thermo Fisher Scientific, Waltham, MA), except for hMSCs, which were detached with TrypLE select (Thermo Fisher Scientific).

N52.E6 cells were propagated in α-MEM (10% fetal bovine serum [FBS], 1x penicillin/streptomycin/glutamine) (Thermo Fisher Scientific).[75]

A549 cells (ATCC # CCL-185) and HepG2 cells (ATCC #HB-8065) were propagated in MEM (10% FBS, 1x penicillin/streptomycin/glutamine) (Thermo Fisher Scientific).

SKOV-3 cells (ATCC # HTB-77) were cultivated in RPMI-1640 Medium (5% FBS, 1x penicillin/streptomycin/glutamine) (Thermo Fisher Scientific).

UM-SCC-11B cells (kindly provided by Prof. Dr. Brunner, Ulm University Medical Center), Huh7 cells (JCRB0403), HEK293T cells (ATCC #CRL-3216), CHO K1 (ATCC #CCL-61), CHO pgsA-745 (ATCC #CRL-2242), and CHO pgsD-677 (ATCC #CRL-2244) were propagated in DMEM (10% FBS, 1x penicillin/streptomycin/glutamine) (Thermo Fisher Scientific).

MiaPaCa cells (ATCC #CRL-1420) were cultivated in DMEM/F12 (10% FBS, 1x GlutaMAX, 1x penicillin/streptomycin) (Thermo Fisher Scientific).

TC31-9C12.C9 hybridoma cells were developed by Laurence Fayadat-Dilman and Wiebe Olijve (Schering Plow Biopharma, Palo Alto, CA) and obtained from the Developmental Studies Hybridoma

Bank, created by the National Institute of Child Health and Human Development of the NIH and maintained at the University of Iowa, Department of Biology. They were propagated in DMEM (10% FBS, 1x penicillin/streptomycin, 1x GlutaMax) (Thermo Fisher Scientific).

MSC isolation and characterization

BM- and A-hMSCs were isolated and characterized to high-quality standard as described previously by Fekete et al.[76] and Rojewski et al.[77]

BM-hMSCs were analyzed for expression (CD105, CD73, and CD90) and lack (CD45, CD34, CD3, and HLA-DQ, -DP, -DR) of specific surface markers, plastic-adherent growth, and trilineage differentiation following the ISCT minimal criteria.[78]

Characterization of A-hMSCs included analysis of expression (CD13, CD105, CD73, CD90) and lack (CD45, CD34, CD14, HLA-DQ, -DP, -DR) of specific surface markers based on the International Federation for Adipose Therapeutics and Science and the International Society for Cellular Therapy joint statement.[79]

Human MSCs were propagated in BioWhittaker Alpha Minimum Essential Medium (Lonza Group AG, Switzerland) supplemented with 5% (A-hMSCs) or 8% (BM-hMSCs)-irradiated pooled human platelet lysate and 500 Units of heparin (Ratiopharm, Ulm, Germany).[80]

HAdV-5 vectors

E1-deleted adenoviral vectors used in this study were based on HAdV-5 (GenBank ID: AY339865.1, sequence from nt 1 to 440 and from nt 3523 to 35,935). All vectors carried a cytomegalovirus promoter-driven EGFP expression cassette in reverse orientation, subcloned from a pEGFP-N1 plasmid (Clontech 6085-1) into the deleted *E1*-region.

The following mutations were introduced using the Red/ET-based homologous recombination kit (GeneBridges, Heidelberg, Germany) and electrocompetent *Escherichia coli* (ElectroMAX DH10B, Invitrogen, Karlsruhe, Germany), according to the manual.

Amino acid sequences for the Hexon HVR1-, HVR5-, and HVR7-modified vectors are listed in (Table 1).

HAdV-5-ΔCAR vector particles additionally carried a point mutation in the fiber knob (Y477A) that significantly reduces CAR-binding.[31]

HAdV-5-Δ5FX vector particles carried 5 point mutations in the hexon protein (I421G, T423N, E424S, L426Y, E451Q) that ablate binding of blood coagulation factor X (FX) to the vector capsid.[72]

HAdV-5/3 carried a chimeric fiber protein, with the fiber knob of HAdV-5 exchanged with the fiber knob of HAdV-3 (European nucleotide archive accession number CAA26029) following the conserved TWLT sequence in the fiber protein.

HAdV-5 vector production and purification

HAdV-5 vectors were produced in *E1*-complementing N52.E6 cells. Cells were infected with a pMOI of 300 to 500 and harvested 48 h post-infection (p.i.). After harvest, cells were resuspended in 50 mM HEPES buffer (pH 7.4) with either 150 mM NaCl (wild-type HVR and HAdV-5-ΔHVR1) or 250 mM NaCl (HAdV5-HexPos2 and -HexPos3 vectors). High salt concentration in the resuspension buffer was used to avoid charge-mediated binding of mutant vector particles to cell debris. After freeze-thaw lysis of cells, cellular nucleic acids were digested using benzonase (Merck KGaA, Darmstadt, Germany). Particles were purified by a CsCl step gradient (density bottom: 1.41 g/mL; density top: 1.27 g/mL; dissolved in 50 mM HEPES, 150 mM NaCl, pH 7.4; 2 h at 176,000 × *g*, 4°C) followed by a continuous CsCl gradient (density: 1.34 g/mL; dissolved in 50 mM HEPES, 150 mM NaCl, pH 7.4; 20 h at 176,000 × *g*, 4°C). Subsequently, particles were desalted using PD-10 size exclusion columns (GE Healthcare, Chicago, IL) and stored at −80°C (storage buffer: 50 mM HEPES, 150 mM NaCl, pH 7.4 with 10% glycerol).

Quality control of all purified vectors included silver staining of SDS-PAGE-separated viral particles, restriction digestion, and sequencing of isolated vector DNA.

Determination of viral titers

Total physical/particle titers were determined by optical density measurement at OD_{260nm} of isolated and denatured vector solutions.[81] pMOI was calculated based on these titers (e.g., pMOI 10 corresponds to 10 viral particles per cell).

Silver staining for viral protein visualization

An amount of 5×10^9 vector particles were mixed with 1x SDS-loading buffer and denatured for 5 min at 70°C. Subsequently, viral proteins were separated by reducing SDS-PAGE (5% stacking gel, 8% separation gel). For visualization, silver staining was performed according to Blum et al.[82]

ZetaSizer measurement

The measurement of the zeta potential was performed with the ZetaSizer Nano-ZS (Malvern, UK); 1×10^{11} vector particles were dialyzed (1×2 h, 1 x overnight, 1×6 h) with 50 mM HEPES (pH 7.4) using the Slide-A-Lyzer Dialysis cassette 3.5K MWCO 0.5 mL (Thermo Fisher Scientific) at 4°C with gentle stirring. Subsequently, glycerol was removed using PD MiniTrap G-25 columns (GE Healthcare) according to the manufacturer's manual but without filter. HAdV-5 vectors with a concentration higher than 1.5×10^9 vector particles/μL were used without exchanging the buffer; 1×10^{11} vector particles were dissolved in 1 mL 50 mM HEPES (pH 7.4) and transferred to a DTS 1070 zeta cell (Malvern). Measurement was performed using the ZetaSizer Nano-ZS (Malvern) at 25°C and analyzed with the DTSNano 5.10 software.

SPR analysis of adenoviral vector binding to immobilized human blood coagulation FX

SPR analysis was performed using the SR7500DC Dual Channel Surface Plasmon Resonance Spectrometer, SR8100 robotic autosampler, SR8600 diverter valve, and SR8500 programmable syringe pump (Reichert Technologies Life Sciences, Buffalo, NY) together with the Autolink software (Reichert Inc.). A CMD500m gold chip (XanTec bioanalytics GmbH, Duesseldorf, Germany) was activated with a 1:1 mixture of 0.1 M 1-ethyl-3-(3-dimethylaminopropyl)carbodiimid (dissolved in H_2O) and 0.1 M Sulfo-NHS (dissolved in 5 mM 2-(N-morpholino)ethanesulfonic acid buffer pH 6) at a flow rate of 25 μL/min for 4 min. Following, human FX (Haematologic Technologies Inc., Essex Junction, VT) was immobilized in 5 mM sodium acetate buffer (pH 4.9) onto the left surface of the chip (120 μg/mL FX, flowrate 10 μL/min for 5 min). Subsequent quenching was performed by injecting 1 M ethanolamine (pH 8.5) on both surfaces of the chip (flowrate 25 μL/min for 4 min). For the analysis of vector binding to FX, 2×10^8 viral particles/μL (diluted in running buffer: 10 mM HEPES buffer with 150 mM NaCl, 5 mM $CaCl_2$ and 0.005% Tween 20, pH 7.4) were injected (25 μL/min for 5 min). For regeneration of the chip, 10 mM HEPES buffer with 150 mM NaCl, 3 mM EDTA and 0.005% Tween 20 (pH 7.4) was used. During SPR analysis, we observed a decrease in chip activity throughout the different analysis cycles, most likely caused by regeneration of the chip with EDTA-containing buffer. Thus, we analyzed the binding of the control wild-type capsid vector HAdV-5 to FX before each vector of interest (which served as a reference).

FX-mediated transduction of SKOV-3 cells

SKOV-3 cells were seeded at 2×10^4 cells/well on nunclon Δ flat-bottom 96-well plates (Thermo Fisher Scientific). The next day, cells were washed with PBS, and 100 μL serum-free medium containing either 0 μg/mL or 8 μg/mL human FX was added. Cells were transduced with a pMOI of 1,000. After 3 h at 37°C, cells were washed with PBS, and serum-containing medium was added; 72 h post-transduction (p.t.), cells were harvested and EGFP expression was analyzed using a CytoFLEX flow cytometer (Beckman Coulter, Brea, CA).

Transduction of cell lines and MSCs

Cell lines (A549, Huh7, MiaPaCa, HepG2, UM-SCC-11B, CHO K1, CHO pgsA-745, CHO pgsD-677) were seeded in nunclon Δ flat-bottom 96-well plates (Thermo Fisher Scientific) at a density of 2×10^4 cells/well. MSCs were seeded in nunclon Δ24-well plates (Thermo Fisher Scientific) at a density of 3×10^4 cells/well. The next day, cells were washed with PBS and transduced with the indicated HAdV-5 vectors at the given pMOI in serum-free medium. For transduction assays with heparin (Ratiopharm) or human lactoferrin (Lf) (Sigma-Aldrich, St. Louis, MO), the respective viral vectors or the cells were incubated with the respective amount of heparin or Lf in serum-free medium at 37°C for 30 min prior to transduction. In case of cell pre-incubation with Lf, cells were washed with PBS three times before transduction. In case of heparinase treatment of cells, cells were treated with the indicated amount of heparinase I or II (New England Biolabs, Ipswich, MA) for 1 h at 37°C in the provided reaction buffer and washed with PBS before transduction. After transduction, cells were incubated at 37°C for 3 h. Subsequently, cells were washed, and serum-containing medium was added; 24 h p.t., cells were harvested and the EGFP expression was analyzed using a CytoFLEX flow cytometer (Beckman Coulter).

HAdV-5 replication assay using HEK293T cells

An amount of 5×10^4 cells of the *E1*-complementing cell line HEK293T were seeded in nunclon Δ 24-well plates (Thermo Fisher Scientific). The following day, cells were infected with pMOI 10, 100, and 1,000. Six days p.i., cells were carefully washed, and subsequently fixed with a 4% paraformaldehyde solution diluted in PBS (Sigma-Aldrich) for 15 min. After washing the fixed cells twice with PBS, cells were stained with a 0.1% crystal violet staining solution dissolved in H_2O (Sigma-Aldrich) for 2 min. After washing twice with PBS, the stained plate was air-dried for some minutes; 100 μL of 100% methanol was added to each well to extract the crystal violet. Then, 1:10 dilutions of the extracted crystal violet were prepared in H_2O and an optical density measurement at 560 nm was performed.

Production of α-Hexon antibody

Antibodies targeting the trimeric adenoviral hexon protein were isolated from TC31-9C12.C9 cell culture supernatant after 96 h of cultivation. The supernatant was incubated with 30 μL Sepharose Protein G beads (Thermo Fisher Scientific) per milliliter of supernatant for 96 h at 4°C. Subsequently, beads were centrifuged at 2000 rpm for 10 min, and the supernatant was discarded. The beads were resuspended in ice-cold P62-BS and transferred into Poly-Prep Chromatography Columns (Bio-Rad Laboratories, Inc., Hercules, CA). After washing twice with 10 mL of ice-cold PBS, the antibodies were eluted from the beads using 0.1 M glycine pH 2.5. The antibody-glycine solution was neutralized immediately by adding 1 M Tris pH 8.0 to a final concentration of 100 mM.

HAdV-5 vector neutralization in naive plasma or by α-hexon IgG

An amount of 2×10^4 A549 cells/well were seeded in nunclon Δ 96-well plates (Thermo Fisher Scientific). The next day, vector particles were incubated with PBS or with different dilutions of HAdV-5-naïve plasma samples for 10 min at 37°C to analyze blood component-mediated neutralization. HAdV-5-naïve human plasma samples were prepared from whole blood by centrifugation at $800 \times g$ for 10 min. To preserve complement activity, blood samples were anticoagulated with 100 μg/mL hirudin (Celgene, Summit, NJ). For analysis of IgG-mediated neutralization, vector particles were incubated with the indicated amounts of α-Hexon IgG antibody in a total volume of 100 μL for 10 min at 37°C. Cells were washed with PBS and transduced with pre-incubated vectors with pMOI 1,000 in 100 μL serum-free medium. After incubation for 3 h at 37°C, cells were washed with PBS and supplemented with 200 μL serum-containing medium. Twenty-four hours p.t., cells were harvested, and EGFP expression was analyzed using a CytoFLEX flow cytometer (Beckman Coulter).

Statistical analysis

Experiments performed in this study were repeated at least three times independently unless described otherwise. Statistical tests used for analysis are stated in the figure legends and were performed using GraphPad Prism software version 8.4.2 (GraphPad Software LLC, San Diego, CA).

Institutional review board statement

This study was performed in accordance with the guidelines of the Declaration of Helsinki and approved by the Ethics Committee of University of Ulm (24/11, 28 July 2011 and 297/14, 25 November 2014).

SUPPLEMENTAL INFORMATION

Supplemental information can be found online at https://doi.org/10.1016/j.omtm.2022.03.004.

ACKNOWLEDGMENTS

The authors acknowledge Cornelia Brunner from the University Medical Center Ulmfor providing the HNSCC cell line UM-SCC-11B.

The work was supported by the German Federal Ministry of Education and Research (BMBF) and the Federal States of Germany Grant "Innovative Hochschule" (FKZ 3IHS024D). Parts of this re-search were funded by the 7th framework programme of the European Commission (project title REBORNE, grant agreement number 241879), the H2020 Programme of the European Commission (project title ADIPOA-2, grant agreement number 643809), and by the Sanitätsakademie der Bundeswehr E/U2AD/ID018/IF557. The materials presented and views expressed here are the responsibility of the authors only. The EU Commission takes no responsibility for any use made of the information set out.

AUTHOR CONTRIBUTIONS

Conceptualization, R.N., S.K., L.K.; methodology, R.N., O.L., C.Q.S, L.K., M.R., H.S; validation, R.N., L.K., and A.K.; formal analysis, R.N.; investigation, R.N., O.L., and C.Q.S.; resources, S.K., M.R., H.S., C.Q.S., P.H.Z., and W.F.; writing—original draft preparation, R.N.; writing—review and editing, R.N., L.K., and S.K.; visualization, R.N.; supervision, S.K., L.K., and A.K.; project administration, S.K.; funding acquisition, S.K. and H.S. All authors have read and agreed to the published version of the manuscript.

DECLARATION OF INTERESTS

The authors declare no competing interests. A patent application has been filed relating to this work by Ulm University (European patent application #19 204,420.4).

REFERENCES

1. Maharlooei, M.K., Bagheri, M., Solhjou, Z., Jahromi, B.M., Akrami, M., Rohani, L., Monabati, A., Noorafshan, A., and Omrani, G.R. (2011). Adipose tissue derived mesenchymal stem cell (AD-MSC) promotes skin wound healing in diabetic rats. Diabetes Res. Clin. Pract. *93*, 228–234.
2. Meinel, L., Hofmann, S., Betz, O., Fajardo, R., Merkle, H.P., Langer, R., Evans, C.H., Vunjak-Novakovic, G., and Kaplan, D.L. (2006). Osteogenesis by human mesenchymal stem cells cultured on silk biomaterials: comparison of adenovirus mediated gene transfer and protein delivery of BMP-2. Biomaterials *27*, 4993–5002.
3. Vural, A.C., Odabas, S., Korkusuz, P., Yar Sağlam, A.S., Bilgiç, E., Çavuşoğlu, T., Piskin, E., and Vargel, İ. (2017). Cranial bone regeneration via BMP-2 encoding mesenchymal stem cells. Artif. Cells Nanomed. Biotechnol. *45*, 544–550.
4. García-Castro, J., Alemany, R., Cascalló, M., Martínez-Quintanilla, J., del Mar Arriero, M., Lassaletta, Á., Madero, L., and Ramírez, M. (2010). Treatment of metastatic neuroblastoma with systemic oncolytic virotherapy delivered by autologous mesenchymal stem cells: an exploratory study. Cancer Gene Ther. *17*, 476–483.
5. Ruano, D., López-Martín, J.A., Moreno, L., Lassaletta, Á., Bautista, F., Andión, M., Hernández, C., González-Murillo, Á., Melen, G., Alemany, R., et al. (2020). First-in-Human, first-in-child trial of autologous MSCs carrying the oncolytic virus Icovir-5 in patients with advanced tumors. Mol. Ther. *28*, 1033–1042.
6. Macrin, D., Joseph, J.P., Pillai, A.A., and Devi, A. (2017). Eminent sources of adult mesenchymal stem cells and their therapeutic imminence. Stem Cell Rev. Rep. *13*, 741–756.
7. Najar, M., Melki, R., Khalife, F., Lagneaux, L., Bouhtit, F., Moussa Agha, D., Fahmi, H., Lewalle, P., Fayyad-Kazan, M., and Merimi, M. (2021). Therapeutic mesenchymal stem/stromal cells: value, challenges and optimization. Front. Cell Dev. Biol. *9*, 716853.
8. Di, G., Du, X., Qi, X., Zhao, X., Duan, H., Li, S., Xie, L., and Zhou, Q. (2017). Mesenchymal stem cells promote diabetic corneal epithelial wound healing through TSG-6-dependent stem cell activation and macrophage switch. Invest. Ophthalmol. Vis. Sci. *58*, 4064–4074.
9. Qi, Y., Jiang, D., Sindrilaru, A., Stegemann, A., Schatz, S., Treiber, N., Rojewski, M., Schrezenmeier, H., Vander Beken, S., Wlaschek, M., et al. (2014). TSG-6 released from intradermally injected mesenchymal stem cells accelerates wound healing and reduces tissue fibrosis in murine full-thickness skin wounds. J. Invest. Dermatol. *134*, 526–537.
10. Rosset, P., Deschaseaux, F., and Layrolle, P. (2014). Cell therapy for bone repair. Orthop. Traumatol. Surg. Res. *100*, S107–S112.
11. Ullah, M., Liu, D.D., and Thakor, A.S. (2019). Mesenchymal stromal cell homing: mechanisms and strategies for improvement. iScience *15*, 421–438.
12. Komarova, S., Kawakami, Y., Stoff-Khalili, M.A., Curiel, D.T., and Pereboeva, L. (2006). Mesenchymal progenitor cells as cellular vehicles for delivery of oncolytic adenoviruses. Mol. Cancer Ther. *5*, 755–766.
13. Moreno, R., Rojas, L.A., Villellas, F.V., Soriano, V.C., García-Castro, J., Fajardo, C.A., and Alemany, R. (2017). Human menstrual blood-derived mesenchymal stem cells as potential cell carriers for oncolytic adenovirus. Stem Cell. Int. *2017*, 3615729.
14. Kumar, S., Chanda, D., and Ponnazhagan, S. (2008). Therapeutic potential of genetically modified mesenchymal stem cells. Gene Ther. *15*, 711–715.
15. Chen, Y.H., Keiser, M.S., and Davidson, B.L. (2018). Viral vectors for gene transfer. Curr. Protoc. Mouse Biol. *8*, e58.
16. Bulcha, J.T., Wang, Y., Ma, H., Tai, P.W.L., and Gao, G. (2021). Viral vector platforms within the gene therapy landscape. Signal. Transduct. Target. Ther. *6*, 1–24.
17. Wold, W.S.M., and Toth, K. (2013). Adenovirus vectors for gene therapy, vaccination and cancer gene therapy. Curr. Gene Ther. *13*, 421–433.
18. Volpers, C., and Kochanek, S. (2004). Adenoviral vectors for gene transfer and therapy. J. Gene Med. *6*, S164–S171.
19. Fougeroux, C., and Holst, P.J. (2017). Future prospects for the development of cost-effective adenovirus vaccines. Int. J. Mol. Sci. *18*, 686.
20. Vujadinovic, M., and Vellinga, J. (2018). Progress in adenoviral capsid-display vaccines. Biomedicines *6*, 81.
21. Choi, J.W., Lee, J.S., Kim, S.W., and Yun, C.O. (2012). Evolution of oncolytic adenovirus for cancer treatment. Adv. Drug Deliv. Rev. *64*, 720–729.
22. Lawler, S.E., Speranza, M.C., Cho, C.F., and Chiocca, E.A. (2017). Oncolytic viruses in cancer treatment a review. JAMA Oncol. *3*, 841–849.
23. Peng, W.-X., and Wang, L. (2017). Adenovirus-mediated expression of BMP-2 and BFGF in bone marrow mesenchymal stem cells combined with demineralized bone matrix for repair of femoral head osteonecrosis in beagle dogs. Cell. Physiol. Biochem. *43*, 1648–1662.

24. Stoff-Khalili, M.A., Rivera, A.A., Mathis, J.M., Banerjee, N.S., Moon, A.S., Hess, A., Rocconi, R.P., Numnum, T.M., Everts, M., Chow, L.T., et al. (2007). Mesenchymal stem cells as a vehicle for targeted delivery of CRAds to lung metastases of breast carcinoma. Breast Cancer Res. Treat. *105*, 157–167.

25. Sonabend, A.M., Ulasov, I.V., Tyler, M.A., Rivera, A.A., Mathis, J.M., and Lesniak, M.S. (2008). Mesenchymal stem cells effectively deliver an oncolytic adenovirus to intracranial glioma. Stem Cells *26*, 831–841.

26. Rincón, E., Cejalvo, T., Kanojia, D., Alfranca, A., Rodríguez-milla, Á., Andrés, R., Hoyos, G., Han, Y., and Zhang, L. (2017). Mesenchymal stem cell carriers enhance antitumor efficacy of oncolytic adenoviruses in an immunocompetent mouse model. Oncotarget *8*, 45415–45431.

27. Nilson, R., Lübbers, O., Weiß, L., Singh, K., Scharffetter-Kochanek, K., Rojewski, M., Schrezenmeier, H., Zeplin, P.H., Funk, W., Krutzke, L., et al. (2021). Transduction enhancers enable efficient human adenovirus type 5-mediated gene transfer into human multipotent mesenchymal stromal cells. Viruses *13*, 1136.

28. Alemany, R., Suzuki, K., and Curiel, D.T. (2000). Blood clearance rates of adenovirus type 5 in mice. J. Gen. Virol. *81*, 2605–2609.

29. Spaeth, E., Klopp, A., Dembinski, J., Andreeff, M., and Marini, F. (2008). Inflammation and tumor microenvironments: defining the migratory itinerary of mesenchymal stem cells. Gene Ther. *15*, 730–738.

30. Ramírez, M., García-Castro, J., Melen, G.J., González-Murillo, Á., and Franco-Luzón, L. (2015). Patient-derived mesenchymal stem cells as delivery vehicles for oncolytic virotherapy: novel state-of-the-art technology. Oncolytic Virotherapy *4*, 149–155.

31. Kirby, I., Davison, E., Beavil, A.J., Soh, C.P.C., Wickham, T.J., Roelvink, P.W., Kovesdi, I., Sutton, B.J., and Santis, G. (2000). Identification of contact residues and definition of the CAR-binding site of adenovirus type 5 fiber protein. J. Virol. *74*, 2804–2813.

32. Parker, A.L., Waddington, S.N., Nicol, C.G., Shayakhmetov, D.M., Buckley, S.M., Denby, L., Kemball-Cook, G., Ni, S., Lieber, A., McVey, J.H., et al. (2006). Multiple vitamin K-dependent coagulation zymogens promote adenovirus-mediated gene delivery to hepatocytes. Blood *108*, 2554–2561.

33. Kalyuzhniy, O., Di Paolo, N.C., Silvestry, M., Hofherr, S.E., Barry, M.A., Stewart, P.L., and Shayakhmetov, D.M. (2008). Adenovirus serotype 5 hexon is critical for virus infection of hepatocytes in vivo. Proc. Natl. Acad. Sci. U S A *105*, 5483–5488.

34. Alba, R., Bradshaw, A.C., Mestre-Francés, N., Verdier, J.M., Henaff, D., and Baker, A.H. (2012). Coagulation factor X mediates adenovirus type 5 liver gene transfer in non-human primates (Microcebus murinus). Gene Ther. *19*, 109–113.

35. Alba, R., Bradshaw, A.C., Coughlan, L., Denby, L., McDonald, R.A., Waddington, S.N., Buckley, S.M.K., Greig, J.A., Parker, A.L., Miller, A.M., et al. (2010). Biodistribution and retargeting of FX-binding ablated adenovirus serotype 5 vectors. Blood *116*, 2656–2664.

36. Mast, T.C., Kierstead, L., Gupta, S.B., Nikas, A.A., Kallas, E.G., Novitsky, V., Mbewe, B., Pitisuttithum, P., Schechter, M., Vardas, E., et al. (2010). International epidemiology of human pre-existing adenovirus (Ad) type-5, type-6, type-26 and type-36 neutralizing antibodies: correlates of high Ad5 titers and implications for potential HIV vaccine trials. Vaccine *28*, 950–957.

37. Sumida, S.M., Truitt, D.M., Lemckert, A.A.C., Vogels, R., Custers, J.H.H.V., Addo, M.M., Lockman, S., Peter, T., Peyerl, F.W., Kishko, M.G., et al. (2005). Neutralizing antibodies to adenovirus serotype 5 vaccine vectors are directed primarily against the adenovirus hexon protein. J. Immunol. *174*, 7179–7185.

38. Chikazawa, M., Otaki, N., Shibata, T., Miyashita, H., Kawai, Y., Maruyama, S., Toyokuni, S., Kitaura, Y., Matsuda, T., and Uchida, K. (2013). Multispecificity of immunoglobulin M antibodies raised against advanced glycation end products: involvement of electronegative potential of antigens. J. Biol. Chem. *288*, 13204–13214.

39. Atasheva, S., Emerson, C.C., Yao, J., Young, C., Stewart, P.L., and Shayakhmetov, D.M. (2020). Systemic cancer therapy with engineered adenovirus that evades innate immunity. Sci. Transl. Med. *12*, 6659.

40. Krutzke, L., Prill, J.M., Engler, T., Schmidt, C.Q., Xu, Z., Byrnes, A.P., Simmet, T., and Kreppel, F. (2016). Substitution of blood coagulation factor X-binding to Ad5 by position-specific PEGylation: preventing vector clearance and preserving infectivity. J. Control. Release *235*, 379–392.

41. Kim, J.S., Lee, S.H., Cho, Y.S., Choi, J.J., Kim, Y.H., and Lee, J.H. (2002). Enhancement of the adenoviral sensitivity of human ovarian cancer cells by transient expression of coxsackievirus and adenovirus receptor (CAR). Gynecol. Oncol. *85*, 260–265.

42. Xu, Z., Qiu, Q., Tian, J., Smith, J.S., Conenello, G.M., Morita, T., and Byrnes, A.P. (2013). Coagulation factor X shields adenovirus type 5 from attack by natural antibodies and complement. Nat. Med. *19*, 452–457.

43. Hammer, K., Kazcorowski, A., Liu, L., Behr, M., Schemmer, P., Herr, I., and Nettelbeck, D.M. (2015). Engineered adenoviruses combine enhanced oncolysis with improved virus production by mesenchymal stromal carrier cells. Int. J. Cancer *137*, 978–990.

44. Lerch, T.F., and Chapman, M.S. (2012). Identification of the heparin binding site on adeno-associated virus serotype 3B (AAV-3B). Virology *423*, 6–13.

45. O'Donnell, J., Taylor, K.A., and Chapman, M.S. (2009). Adeno-associated virus-2 and its primary cellular receptor-Cryo-EM structure of a heparin complex. Virology *385*, 434–443.

46. Hallak, L.K., Spillmann, D., Collins, P.L., and Peeples, M.E. (2000). Glycosaminoglycan sulfation requirements for respiratory syncytial virus infection. J. Virol. *74*, 10508–10513.

47. Waarts, B.L., Aneke, O.J.C., Smit, J.M., Kimata, K., Bittman, R., Meijer, D.K.F., and Wilschut, J. (2005). Antiviral activity of human lactoferrin: inhibition of alphavirus interaction with heparan sulfate. Virology *333*, 284–292.

48. Chen, W., Li, M., Cheng, H., Yan, Z., Cao, J., Pan, B., Sang, W., Wu, Q., Zeng, L., Li, Z., et al. (2013). Overexpression of the mesenchymal stem cell Cxcr4 gene in irradiated mice increases the homing capacity of these cells. Cell Biochem. Biophys. *67*, 1181–1191.

49. Won, Y.W., Patel, A.N., and Bull, D.A. (2014). Cell surface engineering to enhance mesenchymal stem cell migration toward an SDF-1 gradient. Biomaterials *35*, 5627–5635, https://www.sciencedirect.com/science/article/pii/S0142961214003305.

50. Zhang, X., Zhang, C., Tang, T., Qu, Z., Lou, J., and Dai, K. (2008). Immunomodulatory and osteogenic differentiation effects of mesenchymal stem cells by adenovirus-mediated coexpression of CTLA4Ig and BMP2. J. Orthop. Res. *26*, 314–321.

51. Wan, S., Wu, Q., Ji, Y., Fu, X., and Wang, Y. (2020). Promotion of the immunomodulatory properties and osteogenic differentiation of adipose-derived mesenchymal stem cells in vitro by lentivirus-mediated mir-146a sponge expression. J. Tissue Eng. Regen. Med. *14*, 1581–1591.

52. McGinley, L., McMahon, J., Strappe, P., Barry, F., Murphy, M., O'Toole, D., and O'Brien, T. (2011). Lentiviral vector mediated modification of mesenchymal stem cells & enhanced survival in an in vitro model of ischaemia. Stem Cell Res. Ther. *2*, 12.

53. Gabriel, N., Samuel, R., and Jayandharan, G.R. (2017). Targeted delivery of AAV-transduced mesenchymal stromal cells to hepatic tissue for ex vivo gene therapy. J. Tissue Eng. Regen. Med. *11*, 1354–1364.

54. Milone, M.C., and O'Doherty, U. (2018). Clinical use of lentiviral vectors. Leukemia *32*, 1529–1541.

55. Woods, N.-B., Muessig, A., Schmidt, M., Flygare, J., Olsson, K., Salmon, P., Trono, D., von Kalle, C., and Karlsson, S. (2003). Lentiviral vector transduction of NOD/SCID repopulating cells results in multiple vector integrations per transduced cell: risk of insertional mutagenesis. Blood *101*, 1284–1289.

56. Kumar, M., Keller, B., Makalou, N., and Sutton, R.E. (2001). Systematic determination of the packaging limit of lentiviral vectors. Hum. Gene Ther. *12*, 1893–1905.

57. al Yacoub, N., Romanowska, M., Haritonova, N., and Foerster, J. (2007). Optimized production and concentration of lentiviral vectors containing large inserts. J. Gene Med. *9*, 579–584.

58. Dong, J.Y., Fan, P.D., and Frizzell, R.A. (1996). Quantitative analysis of the packaging capacity of recombinant adeno-associated virus. Hum. Gene Ther. *7*, 2101–2112.

59. Alba, R., Bosch, A., and Chillon, M. (2005). Gutless adenovirus: last-generation adenovirus for gene therapy. Gene Ther. *12* (*Suppl 1*), S18–S27.

60. Danthinne, X., and Imperiale, M.J. (2000). Production of first generation adenovirus vectors: a review. Gene Ther. *7*, 1707–1714.

61. Kreppel, F., and Kochanek, S. (2004). Long-term transgene expression in proliferating cells mediated by episomally maintained high-capacity adenovirus vectors. J. Virol. *78*, 9–22.

62. Ebner, K., Pinsker, W., and Lion, T. (2005). Comparative sequence analysis of the hexon gene in the entire spectrum of human adenovirus serotypes: phylogenetic, taxonomic, and clinical implications. J. Virol. *79*, 12635–12642.

63. Carlisle, R.C., Di, Y., Cerny, A.M., Sonnen, A.F.P., Sim, R.B., Green, N.K., Subr, V., Ulbrich, K., Gilbert, R.J.C., Fisher, K.D., et al. (2009). Human erythrocytes bind and inactivate type 5 adenovirus by presenting Coxsackie virus-adenovirus receptor and complement receptor 1. Blood *113*, 1909–1918.

64. Lyons, M., Onion, D., Green, N.K., Aslan, K., Rajaratnam, R., Bazan-Peregrino, M., Phipps, S., Hale, S., Mautner, V., Seymour, L.W., et al. (2006). Adenovirus type 5 interactions with human blood cells may compromise systemic delivery. Mol. Ther. *14*, 118–128.

65. Sumarheni, S., Hong, S.S., Josserand, V., Coll, J.-L., Boulanger, P., Schoehn, G., and Fender, P. (2014). Human full-length coagulation factor X and a GLA domain-derived 40-mer polypeptide bind to different regions of the adenovirus serotype 5 hexon capsomer. Hum. Gene Ther. *25*, 339–349.

66. Bergelson, J.M., Cunningham, J.A., Droguett, G., Kurt-Jones, E.A., Krithivas, A., Hong, J.S., Horwitz, M.S., Crowell, R.L., and Finberg, R.W. (1997). Isolation of a common receptor for coxsackie B viruses and adenoviruses 2 and 5. Science *275*, 1320–1323.

67. Roelvink, P.W., Lizonova, A., Lee, J.G.M., Li, Y., Bergelson, J.M., Finberg, R.W., Brough, D.E., Kovesdi, I., and Wickham, T.J. (1998). The coxsackievirus-adenovirus receptor protein can function as a cellular attachment protein for adenovirus serotypes from subgroups A, C, D, E, and F. J. Virol. *72*, 7909–7915.

68. Kern, A., Schmidt, K., Leder, C., Muller, O.J., Wobus, C.E., Bettinger, K., Von der Lieth, C.W., King, J.A., and Kleinschmidt, J.A. (2003). Identification of a heparin-binding motif on adeno-associated virus type 2 capsids. J. Virol. *77*, 11072–11081.

69. Ranki, T., Kanerva, A., Ristimäki, A., Hakkarainen, T., Särkioja, M., Kangasniemi, L., Raki, M., Laakkonen, P., Goodison, S., and Hemminki, A. (2007). A heparan sulfate-targeted conditionally replicative adenovirus, Ad5.pk7-Δ24, for the treatment of advanced breast cancer. Gene Ther. *14*, 58–67.

70. Xu, D., and Esko, J.D. (2014). Demystifying heparan sulfate–protein interactions. Annu. Rev. Biochem. *83*, 129–157.

71. Bernfield, M., Götte, M., Park, P.W., Reizes, O., Fitzgerald, M.L., Lincecum, J., and Zako, M. (1999). Functions of cell surface heparan sulfate proteoglycans. Annu. Rev. Biochem. *68*, 729–777.

72. Alba, R., Bradshaw, A.C., Parker, A.L., Bhella, D., Waddington, S.N., Nicklin, S.A., Van Rooijen, N., Custers, J., Goudsmit, J., Barouch, D.H., et al. (2009). Identification of coagulation factor (F)X binding sites on the adenovirus serotype 5 hexon: effect of mutagenesis on FX interactions and gene transfer. Blood *114*, 965–971.

73. Zaiss, A.K., Lawrence, R., Elashoff, D., Esko, J.D., and Herschman, H.R. (2011). Differential effects of murine and human factor X on adenovirus transduction via cell-surface heparan sulfate. J. Biol. Chem. *286*, 24535–24543.

74. Bradshaw, A.C., Parker, A.L., Duffy, M.R., Coughlan, L., van Rooijen, N., Kähäri, V.M., Nicklin, S.A., and Baker, A.H. (2010). Requirements for receptor engagement during infection by adenovirus complexed with blood coagulation factor X. PLoS Pathog. *6*, e1001142.

75. Schiedner, G., Hertel, S., and Kochanek, S. (2000). Efficient transformation of primary human amniocytes by E1 functions of Ad5: generation of new cell lines for adenoviral vector production. Hum. Gene Ther. *11*, 2105–2116.

76. Fekete, N., Rojewski, M.T., Fürst, D., Kreja, L., Ignatius, A., Dausend, J., and Schrezenmeier, H. (2012). GMP-compliant isolation and large-scale expansion of bone marrow-derived MSC. PLoS One *7*, e43255.

77. Rojewski, M.T., Lotfi, R., Gjerde, C., Mustafa, K., Veronesi, E., Ahmed, A.B., Wiesneth, M., Körper, S., Sensebé, L.U.C., Layrolle, P., et al. (2019). Translation of a standardized manufacturing protocol for mesenchymal stromal cells: a systematic comparison of validation and manufacturing data. Cytotherapy *21*, 468–482.

78. Dominici, M., Le Blanc, K., Mueller, I., Slaper-Cortenbach, I., Marini, F.C., Krause, D.S., Deans, R.J., Keating, A., Prockop, D.J., and Horwitz, E.M. (2006). Minimal criteria for defining multipotent mesenchymal stromal cells. The International Society for Cellular Therapy position statement. Cytotherapy *8*, 315–317.

79. Bourin, P., Bunnell, B.A., Casteilla, L., Dominici, M., Katz, A.J., March, K.L., Redl, H., Rubin, J.P., Yoshimura, K., and Gimble, J.M. (2013). Stromal cells from the adipose tissue-derived stromal vascular fraction and culture expanded adipose tissue-derived stromal/stem cells: a joint statement of the International Federation for Adipose Therapeutics and Science (IFATS) and the International Society for Cellular Therapy (ISCT). Cytotherapy *15*, 641–648.

80. Fekete, N., Gadelorge, M., Frst, D., Maurer, C., Dausend, J., Fleury-Cappellesso, S., Mailnder, V., Lotfi, R., Ignatius, A., Sensebé, L., et al. (2012). Platelet lysate from whole blood-derived pooled platelet concentrates and apheresis-derived platelet concentrates for the isolation and expansion of human bone marrow mesenchymal stromal cells: production process, content and identification of active components. Cytotherapy *14*, 540–554.

81. Mittereder, N., March, K.L., and Trapnell, B.C. (1996). Evaluation of the concentration and bioactivity of adenovirus vectors for gene therapy. J. Virol. *70*, 7498–7509.

82. Blum, H., Beier, H., and Gross, H.J. (1987). Improved silver staining of plant proteins, RNA and DNA in polyacrylamide gels. Electrophoresis *8*, 93–99.